Highspeed laser ablation cutting of metal

F. Ullmann[1], U. Loeschner[1], L. Hartwig[1], D. Szczepanski[2], J. Schille[1], S. Gronau[1], T. Knebel[1], J. Drechsel[1], R. Ebert[1], H. Exner[1]

[1)] Laser Institute at the University of Applied Sciences, Technikumplatz 17, Mittweida, Germany

[2)] Otto-von-Guericke-Universitaet Magdeburg, Universitaetsplatz 2, Magdeburg, Germany

ABSTRACT

In laser ablation cutting, irradiation of high-intense laser beams causes ejection of molten and evaporated material out of the cutting zone as a result of high pressure gradients, induced by expanding plasma plumes. This paper investigates highspeed laser ablation cutting of industrial grade metal sheets using high-brilliant continuous wave fiber lasers with output powers up to 5 kW. The laser beam was deflected with scan speeds up to 2700 m/min utilizing both a fast galvanometer scan system and a polygon scan system. By sharp laser beam focusing using different objectives with focal lengths ranging between 160 mm and 500 mm, small laser spot diameters between 16.5 µm and 60 µm were obtained, respectively. As a result high peak intensities between $3*10^8$ W/cm² and $2.5*10^9$ W/cm² were irradiated on the sample surface, and cutting kerfs with a maximum depth of 1.4 mm have been produced.

In this study the impact of the processing parameters laser power, laser spot diameter, cutting speed, and number of scans on both the achievable cutting depth and the cutting edge quality was investigated. The ablation depths, the heights of the cutting burr, as well as the removed material volumes were evaluated by means of optical microscope images and cross section photographs. Finally highspeed laser ablation cutting was studied using an intensified ultra highspeed camera in order to get useful insights into the cutting process.

Keywords: highspeed laser ablation cutting, highspeed, cutting, laser, fiber laser, metal, AISI304

1. INTRODUCTION

First results achieved in highspeed laser cutting have been presented in the beginning of the 1990´s [1,2]. Thin sheet parent material with a thickness less than 0.5 mm was cut through with a cutting speed up to 300 m/min using a CO_2 laser. In addition for 0.35 mm thick magnetic steel sheets a cutting speed of 140 m/min has been demonstrated. However, these speeds were obtained for linear cutting, but in fast contour cutting high dynamic machining systems are essential, which allow the rapid change of cutting directions while the cutting speed remains constant. Laser scan systems can fulfill these requirements because of considerably faster beam deflection speeds can be achieved due to the small masses of scan mirrors which have to be moved. The latest generations of galvanometer scanners and polygon scanners are able to deflect high-brilliant laser beams delivered by fiber laser systems and disc laser systems. As a result, highspeed laser ablation cutting as well as remote fusion cutting can be performed with laser output powers of several kilowatts. Thus the impinging intensities are sufficiently high enough for effective material removal and, in contrast to conventional laser cutting a supporting process gas is not required. Furthermore, the processing speed can be considerably increased due to very fast beam deflection relative to the material surface by galvanometer scanner or polygon scanner systems without any movement neither of the cutting head nor the work piece.

An overview on remote cutting technology and conventional cutting technologies is given in [3]. Highspeed laser ablation cutting as a remote cutting technology describes a combination of sublimation cutting and fusion cutting using multiple passes of a laser beam across the work piece (scans) until the material is cut through via ablation of a comparatively small amount of material. In a first study the separation of thin metal sheets using laser remote cutting techniques has been successfully demonstrated [4]. In remote fusion cutting the material will be cut through at once using melt pressure. In comparison, the maximum processing speed for highspeed ablation cutting is currently around 2000 m/min per scan and for remote fusion cutting 15 m/min are demonstrated [5].

High-Power Laser Materials Processing: Lasers, Beam Delivery, Diagnostics, and Applications II, edited by Friedhelm Dorsch, Proc. of SPIE Vol. 8603, 860311 © 2013 SPIE
CCC code: 0277-786X/13/$18 · doi: 10.1117/12.2006205

This paper discusses the impact of the mainly ablation process influencing parameters on highspeed laser ablation cutting, such as laser power, scan speed, focus spot size, intensity of laser radiation, and energy input per unit length. The quality of the cutting edges as well as the geometrical dimension of the cutting kerfs was evaluated by means of SEM and digital optical microscope photographs. Finally highspeed laser cutting was investigated by using a highspeed camera providing useful insights into the cutting process.

2. EXPERIMENTAL DETAILS

Highspeed laser ablation cutting was investigated on stainless steel X5CrNi 18-10 (AISI 304) using two different single mode fiber lasers made by IPG. The lasers operated in continuous mode at the wavelength of 1070 nm with a maximum output laser power of 3 kW and 5 kW, respectively. In addition the utilized laser machining station was equipped with a galvanometer scanner Superscan SC 30 (Raylase AG) and a polygon scanner with a diameter of 10 inches (Lincoln laser). The maximum ratings of the applied processing parameters are summarized in table 1.

Table 1: Laser processing parameters.

focal lenght [mm]		160	230	330	500
laser spot size d_{86} [µm]		16.5	21	32	60
max. laser power onto work piece P_{cw} [kW]		2.65	4.3		
max. intensity onto work piece I_{max} [W/cm²]		$2.5*10^9$	$2.5*10^9$	$1.1*10^9$	$3.0*10^8$
max. scan speed v_{sc} [m/min]	galvanometer scanner	900	1200	2100	2700
	polygon scanner	-	2250	-	-

The irradiation regime consisted of a number of line scans with up to 50 mm in length whereas the focal plane was coincident with the sample surface. The shift of the focal position of the laser beam, as reported previously in high brilliance laser processing [6], was avoided by a delay of one second between consecutive laser beam passes. The quality of the cutting edge was estimated by SEM micrographs. The depths and the clear cross sectional area of the cutting kerfs were evaluated by means of digital optical microscope images taken from cross-section polishes. In addition, burr formation at the cutting edge was characterized quantitatively too. In addition an intensified highspeed camera system (HSFC-Pro, PCO AG) was used in order to get information on the cutting process.

3. RESULTS AND DISCUSSION

Initially the ablation depth was evaluated with respect to the laser beam spot size, the impinging laser power, and scan speed using the galvanometer scanner. The ablation depth is determined by the material thickness which can be cut through. Figure 1 presents a set of cutting kerfs achieved with increasing number of scans. Whereas a V-shaped kerf has been obtained as a result of a single scan laser ablation (figure 1a), the cutting kerfs have been transformed in a U-shape with increasing number of scans. In addition molten and resolidified material was deposited at the cutting kerf walls, induced by melt ejection as a result of intense plasma formation within the cutting kerf. Accordingly figure1b) indicates single layers of solidified material close to the entrance of the cutting kerf, but with increasing ablation depth the constriction of the cutting kerf is clearly recognizable (figure 1c).

The maximum kerf width of 200 µm was obtained with only little numbers of scans and a small ablation depth, respectively. Furthermore it was observed that the width at the entrance of the cutting kerf varied greatly between several 10 µm and 100 µm with increasing ablation depth, caused by massive melt deposition. As a result the kerf width has been assessed inconclusive and thus it was not taken into discussion as significant evaluation parameter. In consequence laser ablation cutting is evaluated by the volume ablation rate, determined based on the clear cross section area of the cutting kerf. Indeed, the volume ablation rate is basically influenced by melt deposition too, but the volume ablation is stronger affected by the ablation depth instead of the kerf width. Maximum values are presented later on.

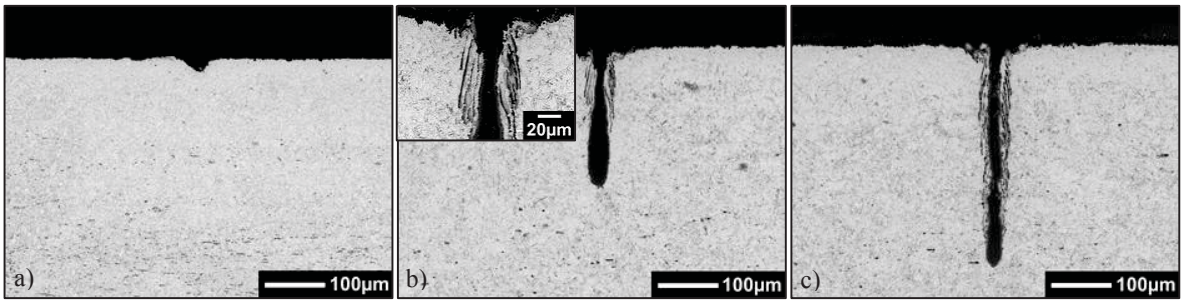

Figure 1: Cross section photographs of cutting kerfs obtained with various number of scans, parameters: P_{cw} = 0.86 kW, d_{86} = 21 µm, v_{sc} = 1200 m/min; a) 1 scan, b) 10 scans, c) 20 scans.

Figure 2 presents the ablation depth as a function of the number of scans, obtained using a scan speed of 900 m/min, a spot size of 21 µm, and various laser powers ranging between 0.43 kW and 4.3 kW. As it can be seen, initially, the ablation depth increases almost linear with increasing number of scans. With higher scan numbers the curve shape becomes more and more degressive, and finally tends to stagnate at a certain number of scans. For instance, as achieved in ablation cutting using a laser power of 0.43 kW, the ablation depth stagnates at 200 µm above a number of 10 scans. With the double laser power of 0.86 kW and more than 30 scan numbers the ablation depth increases insignificantly tending toward the ablation depth limit of 600 µm. Moreover, two effects have been identified which mainly influence the quantity of material removal with regard to the ablation efficiency: vaporization of material in combination with plasma formation and melt ejection out of the cutting kerf due to plasma pressure. Further the results obtained indicate that a higher intensity of the incident laser beam, controlled by the laser power, enhanced the degree of material vaporization. As a result the plasma pressure rises, accompanied by a higher amount of molten material ejected out of the cutting kerf. Thus, a higher laser power level supports the ablation process leading to an increase in ablation depth. But, melt ejection is hindered when a distinctive ablation depth is reached due to re-solidification of melt at the walls of the cutting kerfs. According to that the more degressive course of the ablation depth at larger number of scans indicates the lower efficiency of the ablation process at deeper ablation depths.

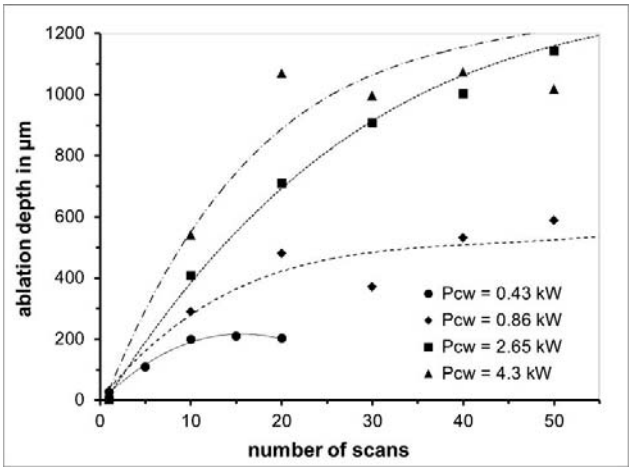

Figure 2: Ablation depth vs. number of scans for various laser power levels, parameters: d_{86} = 21 µm, v_{sc} = 900 m/min.

The maximum ablation depth achieved within the investigated parameter set was in the range of 1 mm. As can be derived from figure 2, an ablation depth of 1 mm can be achieved either with a laser power of 4.3 kW and 20 scans or a laser power of 2.65 kW and 40 scans. In conclusion, the cumulative cutting speed as the scan speed divided by the applied number of scans is 45 m/min for 20 scans at a laser power of 4.3 kW. But the cumulative cutting speed is only the half at the lower laser power and 40 scans, despite the considerably higher total incident laser power as the product of the laser power and scan number. This result supports the assumption made above that the level of plasma induced

depending on the laser power will affect the ablation process. Furthermore, for an ablation depth of 0.5 mm and an applied laser power of 4.3 kW the cumulative cutting speed could be increased to 97 m/min. Thus, the cumulative cutting speed is above the maximum speed of 75 m/min obtained with a laser power of 2.65 kW as reported in [7] and even exceeds the theoretical limit for remote cutting of 60 m/min, proposed in [8].

Figure 3 depicts the ablation depth as a function of the cumulative energy input per unit length. The energy input per unit length can be calculated by dividing the applied laser power by the scan speed. Because of multiple scans performed in highspeed ablation cutting the energy input per unit length multiplied by the respective number of scans can be understood as the cumulative energy input per unit length. From the plot a linear correlation between the ablation depth and

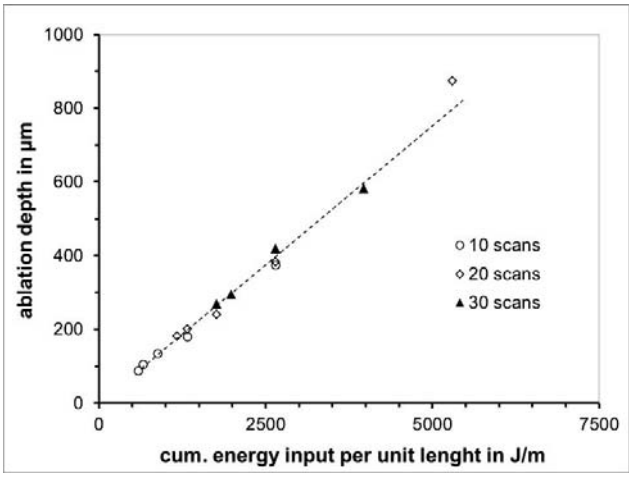

Figure 3: Ablation depth vs. cumulated energy input per unit length for various number of scans, parameters: P_{cw} = 2.65 kW, d_{86} = 60 µm, varied scan speed.

the cumulative energy input per unit length, calculated for a laser power of 2.65 kW and a spot size of 60 µm but varied scan number and scan speed, can be derived. That means, for a given ablation depth of 400 µm for example, a cumulative energy input per unit length of 2650 J/m is required. This value can be generated either with 10 scans and a scan speed of 600 m/min or 20 scans and a scan speed of 1200 m/min or even 30 scans at a scan speed of 1800 m/min, resulting in the same cumulative cutting speed of 60 m/min.

To exploit the maximum scan speed, an objective with a focal length of 500 mm was attached to the galvanometer scanner. In the diagram in figure 4 the ablation depth is plotted as a function of the scan speed, obtained using different number of scans at a laser power of 2.65 kW and a spot size of 60 µm. For a given number of scans the ablation depth in-

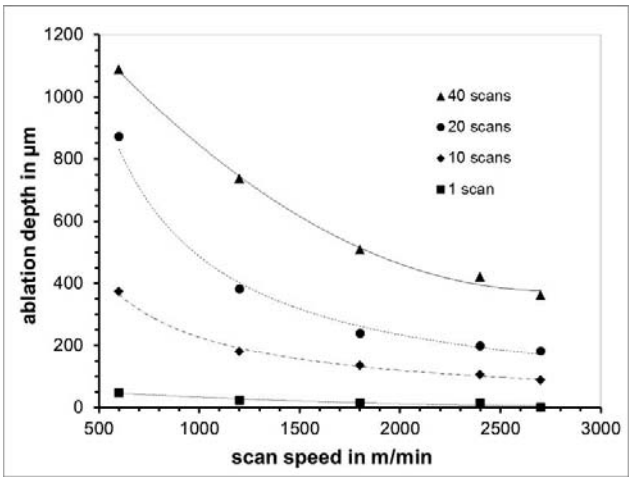

Figure 4: Ablation depth vs. scan speed for different number of scans, parameters: P_{cw} = 2.65 kW, d_{86} = 60 µm.

creases with decreasing scan speed due to higher energy input per unit length. Furthermore, the dwell time, defined as the time interval while the laser beam is moved for a distance corresponding to its spot size, grows from 1.3 ms up to 6 ms when scan speed is lowered from 2700 m/min down to 600 m/min. So it can be assumed, that heat penetration into the material due to heat conduction becomes more pronounced, accompanied by a more intensive material melting. Following, the melt will be ejected by plasma pressure. In conclusion, with lower scan speeds the ablation process is characterized by an increased melt ejection. This hypothesis will be supported by highspeed camera recordings discussed below.

Figure 5 demonstrates the influence of different combinations of spot size and laser power on the ablation depth as a function of the number of scans for two given scan speeds while the intensity of laser radiation remains constant. For the respective scan speeds of 600 m/min and 900 m/min a combination with higher laser power and larger spot size result in a more effective ablation process, but the individual influence of laser power and spot size on the ablation depth cannot be separated.

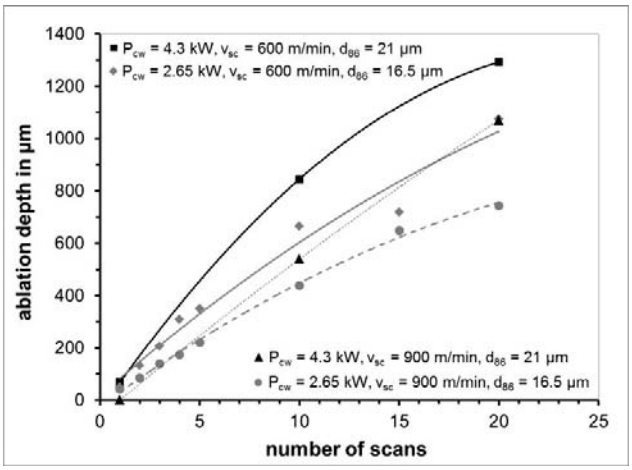

Figure 5: Ablation depth vs. number of scans for a given intensity of laser radiation of $2.5*10^9$ W/cm² realized with different combinations of spot size and applied laser power for scan speeds of 600 m/min and 900 m/min.

In order to clarify the influence of the spot size on the ablation depth the spot size was varied while laser power and scan speed were held constant. Figure 6 shows the influence of the spot sizes in respect to the achievable ablation depth obtained at a scan speed of 600 m/min and a laser power of 2.65 kW. The focal length of the objectives, spot sizes, and respective intensity values are listed in table 2.

Table 2: Focal length and laser parameters used for comparison of spot sizes.

focal lenght [mm]	160	230	330	500
measured laser spot size d_{86} [µm]	16.5	21	32	60
max. laser power onto work piece P_{cw} [kW]	2.65			
max. intensity onto work piece I_{max} [W/cm²]	$2.5*10^9$	$1.5*10^9$	$0.7*10^9$	$0.2*10^9$

As can be seen with smaller spot size and therefore higher intensity of laser radiation the ablation depth is increased. At higher intensity first a larger portion of material will be vaporized leading to a stronger plasma formation, resulting secondly in a more effective melt ejection out of the ablation kerf as discussed before. For example, at a given number of 10 scans the ablation depth can be increased by 80% if the spot size is reduced from 60 µm down to 16.5 µm corresponding to a rise in intensity of laser radiation by a factor of 13.

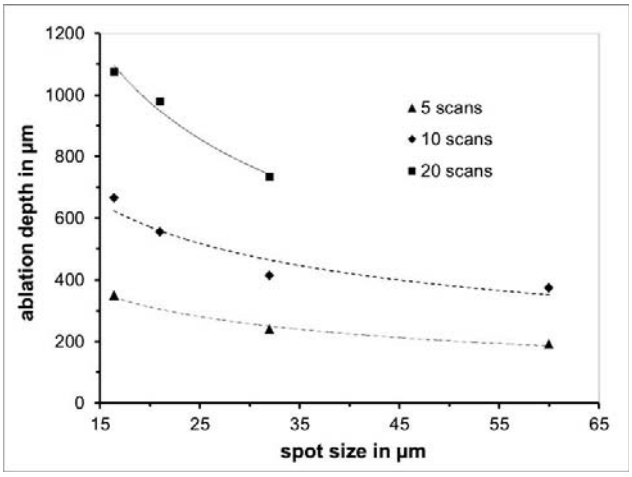

Figure 6: Ablation depth vs. number of scans at different spot sizes, parameters: P_{cw} = 2.65 kW, v_{sc} = 600 m/min.

By using the polygon scanner in combination with the given objectives, considerably higher scan speeds can be realized in contrast to the galvanometer scanner, allowing to investigate the impact of the scan speed in greater detail. In figure 7 for two different spot sizes 21 µm and 60 µm the ablation depth is plotted against the number of scans for almost comparable scan speeds and laser powers of 2400 m/min and 2250 m/min as well as 1.84 kW and 1.65 kW, respectively. Although the parameters are slightly different, the energy input per unit length related to one scan still remains constant. In order to realize a scan speed of 2400 m/min with a spot size of 21 µm, the objective with a focal length of 230 mm was attached to the polygon scanner. Deduced from the graph shown in figure 7 the achieved ablation depth at a given number of scans is considerably larger if the smaller spot size is applied. At a number of 40 scans for instance, a rise of 40% can be determined. Hence, at given laser power and scan speed the efficiency of the ablation process increases with smaller spot sizes and therefore higher intensity of laser radiation. In addition, a less efficient ablation process with growing number of scans can be observed too. Thus the results achieved by using the polygon scan system are conclusive to the results presented above for the galvanometer scanner.

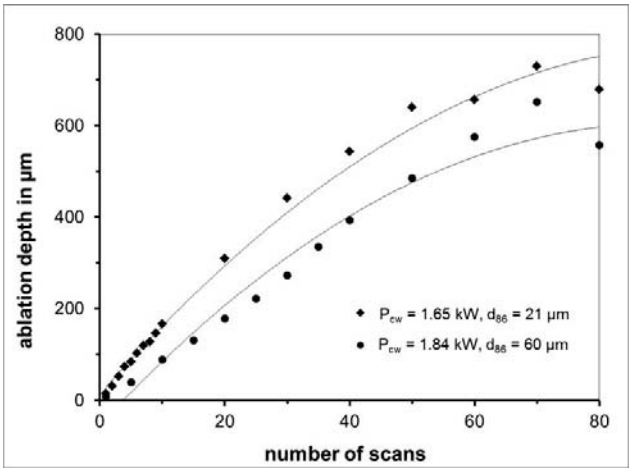

Figure 7: Ablation depth vs. number of scans for two spot sizes, parameters: P_{cw} = 1.65 kW and: P_{cw} = 1.84 kW, v_{sc} = 2250 m/min and v_{sc} = 2400 m/min.

In conclusion, within the investigated parameter range the maximum ablation depth as representative material thickness which can be reliable cut through is 1.4 mm. Appropriate parameter sets to achieve the maximum depth are listed in table 3. It can be seen that for a given scan speed and laser power level, the fastest cumulative cutting speed is achieved with the smallest spot size.

Table 3: Parameter sets for an ablation depth of 1.4 mm.

laser power onto work piece P_{cw} [kW]	2.65		4.3		
focal lenght [mm]	160	330	230	330	500
measured laser spot size d_{86} [µm]	16.5	32	21	32	60
scan speed [m/min]	600				
number of scans	30	50	20	30	40
cumulative cutting speed [m/min]	20	12	30	20	15

Further the volume ablation rate was affected by the process parameters scan speed and laser power. For example, for a given laser power of 4.3 kW and a spot size of 21 µm a maximum ablation volume rate of 2700 mm³/min per scan was achieved for the lowest applied scan speed of 600 m/min and 10 scans. Because of the degressive course of ablation depth with increasing number of scans the volume ablation rate per scan was lowered. The increase of the scan speed up to 1,200 m/min, but apart from that, constant processing parameters the volume ablation rate reduced to 2200 mm³/min. As expected, the volume ablation rate increases with higher laser power.

The quality of the cutting edge is primarily characterized by burr formation and surface appearances of the cutting edge. By analyzing the burr formation, at the top site of the cutting kerf a considerable amount of burr can be observed originating from resolidified melt, but the bottom of the kerf is almost melt-free, shown in figure 8. For a given laser power and spot size the burr height is influenced by scan speed and number of scans. Initially, the height of burr increases rapidly up to 10 scans. Afterwards the growth of burr becomes more and more degressive, and at a number of 20 scans it tends to stagnate because of the melt is ejected less efficient with increasing ablation depth and growing burr, respectively. By discussing the influence of the scan speed, the results show a tendency to larger heights of burr if lesser scan speed is used, see figure 10. For a given laser power of 2.65 kW, a spot size of 60 µm, and a scan speed of 2700 m/min for example, the height of burr rises up to 50 µm within the first 10 scans and stagnates then at 70 µm with further increase of the number of scans. If the scan speed is reduced to 600 m/min, the height of burr is already 95 µm after 10 scans and it tends to stagnate at 110 µm. Hence, lower scan speed is accompanied by stronger burr formation because of increased melt ejection as discussed above. Additionally, there is a tendency to reduced burr formation in the order of 20-30% by using smaller spot sizes due to higher intensities of laser radiation and therefore an increased degree of material evaporation.

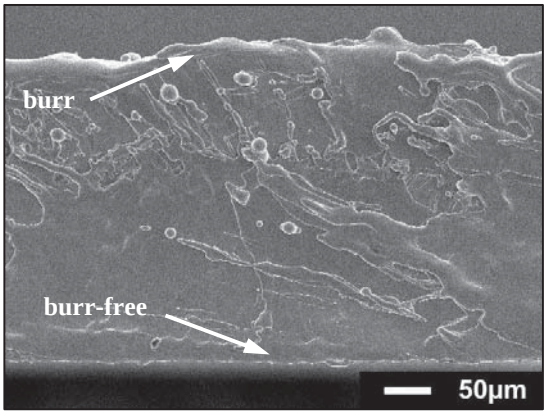

Figure 8: SEM micrograph of the cutting edge, parameters: P_{cw} = 1.8 kW, d_{86} = 16.5 µm, v_{sc} = 600 m/min, 5 scans.

Figure 9 shows cutting edges obtained on a 0.3 mm thick stainless steel sheet by using different parameter sets. Basically, the roughness of cutting edges generated by the ablation cutting process is significantly increased in comparison to those produced with conventional CO_2 laser cutting technology [9]. In figure 9 a) an applied laser power of 0.62 kW and a number of 28 scans and in figure 9 b) 6 scans with a laser power of 1.76 kW were necessary to cut through. Comparing the surface qualities, the surface in the left SEM micrograph appears rough with bulgy areas of molten and resolidified

melt and some melt droplets, whereas the cutting edge in the right SEM micrograph looks considerably smoother and is covered with a thin molten film. Additionally, burr formation is reduced. In discussion, less laser power results in reduced intensity of laser radiation followed by a smaller degree of vaporization accompanied by inefficient melt ejection (figure 9a). This effect will be more apparent in laser processing using a comparatively higher number of scans. But in

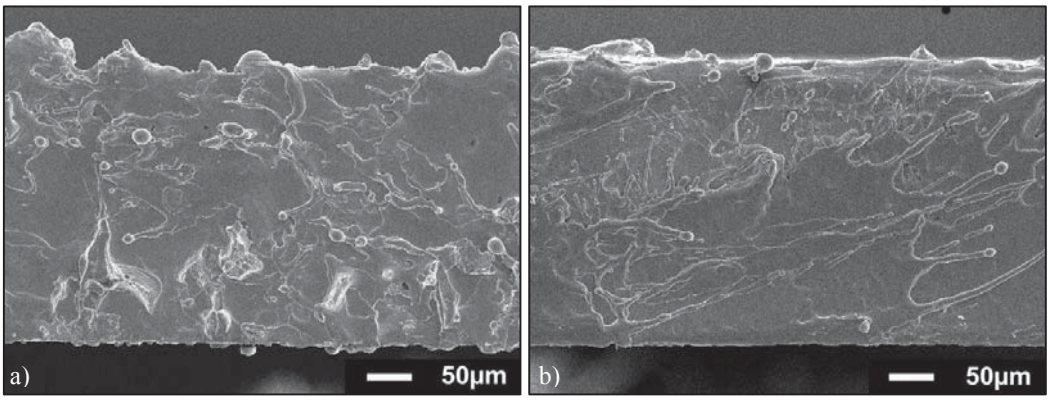

Figure 9: SEM micrographs of cutting edges, parameters: d_{86} = 21 µm, v_{sc} = 600 m/min, sheet thickness 0.3 mm, a) P_{cw} = 0.62 kW, 28 scans; b) P_{cw} = 1.76 kW, 6 scans.

case of higher laser power, a considerably greater proportion of material can be evaporated. Furthermore the results indicate that melt ejection out of the cutting kerf is much more efficient due to higher plasma pressure (figure 9b). The described material ablation behavior has been observed for all spot sizes.

However, as known from conventional laser cutting, the edge quality is considerably influenced by the cutting speed. In figure 10 a set of cutting edges produced with various scan speeds are presented. It can be seen, that roughness is reduced

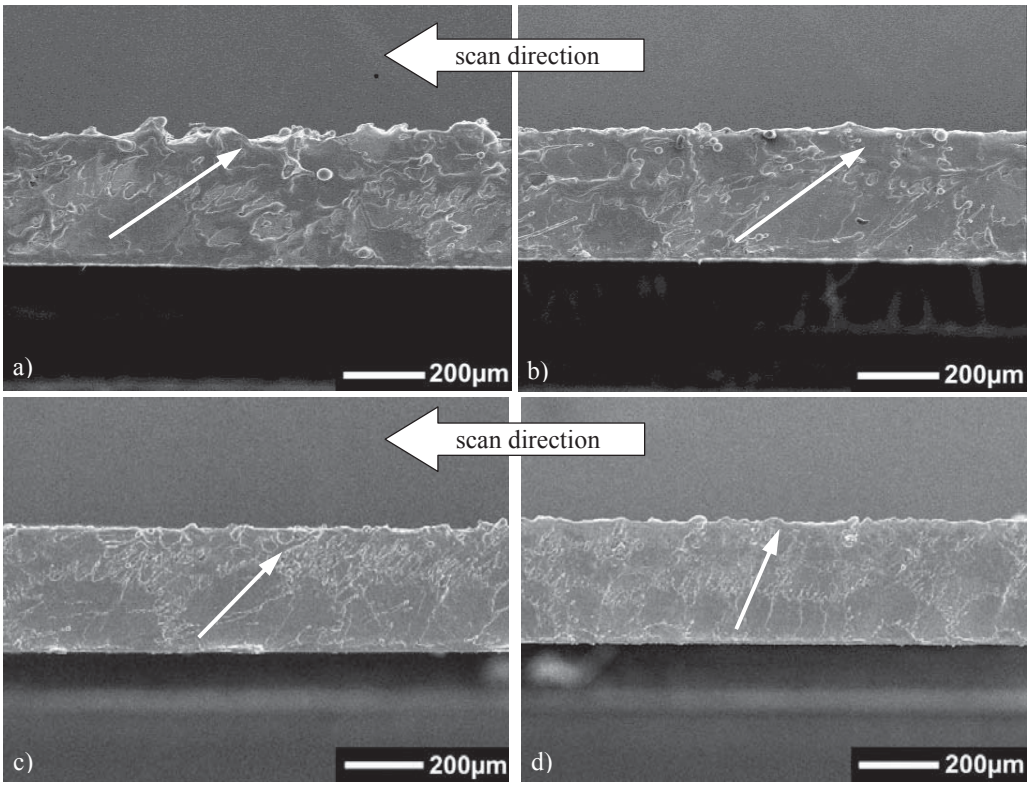

Figure 10: SEM micrographs of cutting edges for various scan speeds, parameters: P_{cw} = 0.94 kW, d_{86} = 32 µm, a) v_{sc} = 480 m/min, 8 scans, b) v_{sc} = 600 m/min, 9 scans, c) v_{sc} = 900 m/min, 13 scans, d) v_{sc} = 1800 m/min, 22 scans.

with higher scan speed. At the same time, burr formation is dropping. The improved edge quality can be attributed to a gradually shorter dwell time of the laser spot at a certain position of the material if scan speed is rising. Therefore, heat penetration into the material, which is responsible for extensive melting, becomes more and more insignificant as explained above. Thus, if improved edge quality is required, increased scan speed should be applied although the ablation depth per scan is reduced leading to larger number of scans.

Having a closer look to the cutting edges it can be seen, that the preferred orientation of the melt flow is affected by the scan speed. In the ablation cutting process with continuous wave laser radiation a melt front can be assumed in scan direction as demonstrated in the schematic diagram in figure 11. It becomes evident, that the inclination angle of the melt front normal in respect to the direction of the incident laser beam depends on the ratio of spot size and ablation depth. That means, with reduced ablation depth observed at rising scan speed the inclination angle is dropping. For the parameter sets used for cutting results presented in figure 10 the inclination angle was calculated from spot size and the respective average ablation depth per scan. By drawing the inclination angle into the SEM micrographs in figure 10, the preferred orientation of melt flow and the inclination angle of the melt front normal agree very well. In discussion, melt flow and melt ejection will be caused by confining plasma pressure. But, due to an inclined melt front, melt flow is preferred orientated to the melt front normal, shown in figure 11.

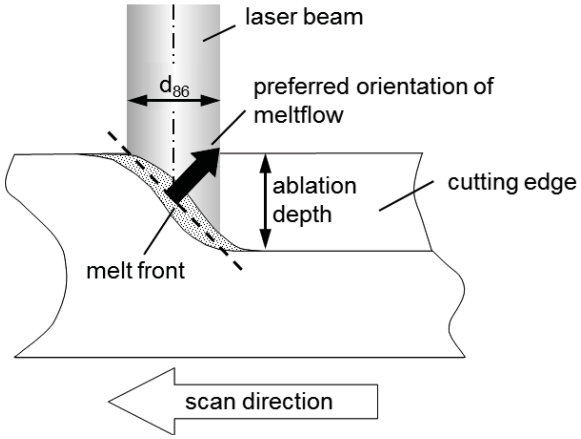

Figure 11: Schematic of the melt front formation in laser ablation cutting.

During highspeed cutting experiments highspeed camera images were recorded in order to get information from highspeed cutting process. Figure 12 depicts the plasma formation during the cutting process for different scan speeds. It is remarkable, that the plasma plume appears to be inclined in respect to the direction of the incident laser beam. Furthermore, it seems that the plasma plume straightens up with rising scan speed. Although there can be presumed comparable

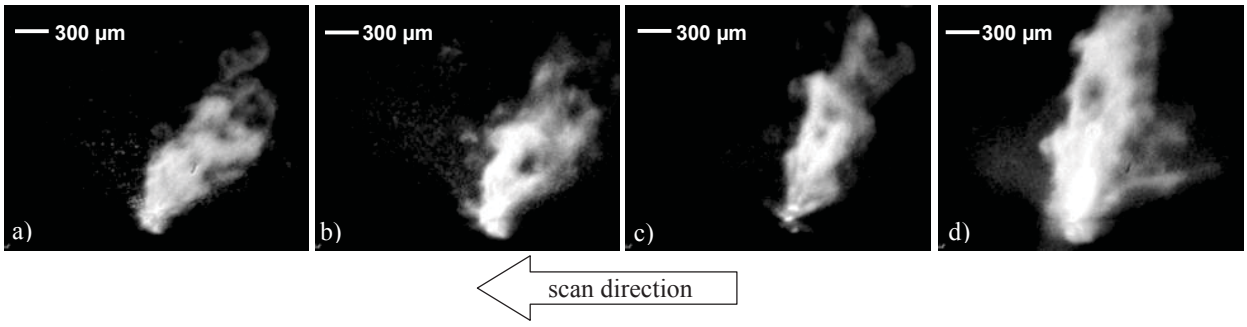

Figure 12: Highspeed camera recordings at various scan speeds, parameters: P_{cw} = 1.7 kW, d_{86} = 21 µm, a) v_{sc} = 240 m/min, b) v_{sc} = 360 m/min, c) v_{sc} = 480 m/min, d) v_{sc} = 900 m/min.

tendencies of inclination in respect to figure 10, the exact angles of inclination were not in accordance at comparable scan speeds. Under the condition of an equivalent rate of expansion of the plasma plume, an increased inclination in

respect to the direction of the incident laser beam should be expected with rising scan speed. This is because of portions of plasma within the plasma plume originating from previous ablated material in the cutting process, which suggests an inclined plume. Thus, the observed stages of inclination cannot be attributed to varying scan speeds at first glance. There are further investigations necessary to understand the described effect. Besides, the size of particles nearby the plasma plume was considerably increased when scan speed was reduced indicating a higher degree of melt formation for lower scan speeds as discussed in relation to figure 4 and observed in figure 10.

4. CONCLUSIONS

In this paper results on highspeed laser cutting of steel are presented. The impact of important process parameters on the achievable ablation depth was investigated in detail. The ablation depth and thus, the material thickness which can be cut through strongly depend on the process parameters laser power, scan speed, spot size, and number of scans. Thereby, the ablation depth per scan in combination with applied scan speed defines the efficiency of the cutting process represented by the cumulative cutting speed for a certain sheet thickness. The ablation depth can be increased by raising laser power, by reducing spot size, or by dropping scan speed. But, considering cutting edge quality higher scan speed should be applied resulting in reduced burr formation and smoother cutting edges.

Based on these facts a cumulative cutting speed of up to 97 m/min can be realized for a given sheet thickness of 0.5 mm and an applied laser power of 4.3 kW. The maximum sheet thickness which can be reliable cut through within the investigated parameter range is 1.4 mm. For this, a maximum cumulative cutting speed of 30 m/min was gained.

Highspeed camera recordings reveal information from the cutting process. Plasma plume formation seems to be inclined in respect to the direction of the incident laser beam. The angle of inclination depends on applied scan speed. Also, in accordance to the observed cutting edge quality, for lower scan speed the particle size nearby the plasma plume appears increased indicating a higher degree of molten material.

ACKNOWLEDGMENT

The authors gratefully acknowledge financial support of the presented work by the Federal Ministry of Education and Research (project number 03IPT506X).

REFERENCES

[1] Preißig, K. U. and Albrecht, J., “Hochgeschwindigkeitsschneiden von Feinstblechen mit Lasern. Qualitaetsverbesserung / High-speed cutting of finest sheet by lasers. Quality improvement“, Journal Baender, Bleche, Rohre 33, 79-88 (1992).

[2] Preißig, K. U., Petring, D. and Herziger, G.,“High speed laser cutting of thin metal sheets“, Proc. of SPIE 2207, 96-110 (1994).

[3] Zaeh, M. F., Moesl, J., Musiol, J. and Oefele, F., “Material processing with remote technology - revolution or evolution?”, Physics Procedia 5, 19-33 (2010).

[4] Himmer, T., Pinder, T., Morgenthal, L. and Beyer, F., “High brightness laser in cutting application”, Proc. of ICALEO, 87-91 (2007).

[5] Szczepanski, D. and Juettner, S., ”Hochgeschwindigkeitlaserschneiden duenner Bleche für Anwendungen im Elektroantrieb”, Proc. of IMWK, 25-28 (2012).

[6] Eiselen, S., Zapf, H., Mantel, E., Hofmann, L. and Schmidt, M., “Impact of thermal focal shift on laser cutting processes with high brightness lasers”, Proc. of ICALEO, 282-291 (2012).

[7] Hartwig, L., Ebert, R., Kloetzer, S., Weinhold, S., Drechsel, J., Peuckert, F., Schille, J. and Exner, H., “Material processing with a 3kW single mode fibre laser”, JLMN-Journal of Laser Micro/Nanoengineering Vol. 5, No. 2, 128-133 (2010).

[8] Petring, D., “Calculable laser cutting”, Proc. of LIM, 209-214 (2009).

[9] Pihlava, A., Purtonen, T., Salminen, A., Kujanpaeae, V., Hartwig, L. and Schille, J., “Quality of Remote Cutting”, Proc. of ICALEO, 354-361 (2010).